EXPERIMENTAL STUDY ON DEFORMATION PROPERTIES OF UNSATURATED COMPACTED SOIL BASED ON DIGITAL IMAGE MEASUREMENT

J. Dong[1,2*] – L. Shao[2]

[1]Department of Civil Engineering, College of Mining Engineering, Liaoning Technical University, Huludao 125105, China
[2]Stake Key Laboratory of Structural Analysis for Industrial Equipment, Dalian University of Technology, Dalian 116024, China

ARTICLE INFO

Abstract:

Due to the end restraint or the restraint of contact transducers to sample deformation, the results of conventional strain measurement method can not reflect the properties of sample deformation comprehensively. The digital image measurement method can measure the deformation of overall and local sample non-intrusively and selectively and can overcome some shortcomings of using conventional strain measurement method for unsaturated soil sample in suction-controlled triaxial tests. The deformation measurement results of unsaturated compacted soil samples show that the end restraint has significant effect on the deformation of the sample. The deformation properties of middle 1/3 sample are evidently different from those of the overall sample that is affected by the end restraint in suction-controlled isotropic loading and triaxial compression tests. The deformation measurement results of middle 1/3 sample can really correspondingly reflect basic deformation properties of unsaturated soil and study a constitutive model preferably.

1 Introduction

Studies on unsaturated soils are usually based on laboratory experiments conducted on compacted and reconstituted soils in suction-controlled triaxial tests. Displacement transducer and contact transducer are usually used for the axial strain and radial strain measurement in unsaturated soil triaxial test, respectively, such as Hall Effect Transducer and Local Displacement Transducer. But those contact transducers can incur restraints on radial deformation of samples. Additionally, the contact transducers can measure only a few radial sections of samples due to bulk of self and sample. As a result, the measurement cannot reflect local properties of sample deformation comprehensively [1-2]. In the past decade, development of digital image measurement has been applied to deformation measurement of sample in soil triaxial test, which solved the deficiency of contact transducer commendably. For example, Shao et al. [3-5] developed computer digital image

---

measurement technique of soil sample deformation in triaxial test, and provided a new experimental approach for deformation measurement of sample in unsaturated soil triaxial test. Their method can measure the deformation of middle sample non-intrusively such that the end restraint effect is lessened by adopting the digital image measurement method in suction-controlled unsaturated soil triaxial test. Moreover, the deformation process of the unsaturated soil sample can be recorded and analyzed after the tests have been done. In this paper, we studied a sub-pixel accurate corner locator approach for deformation measurement of sample in soil triaxial test [6-7] and suction-controlled unsaturated soil triaxial test to study the effect of end restraint on deformation properties of unsaturated compacted soil.

2 System Composition and Principle of Measurement

2.1 System composition

The digital image measurement system based on sub-pixel corner locator method is composed of a USB 2.0 CMOS camera (resolution 1280×1024 px), a computer, and digital image processing software, as shown in Fig. 1. Apparatus of soil triaxial test were improved as follows, Fig. 1: (a) the black rubber membranes, on which white square marks were printed, were used to wrap samples; (b) the structure of each cell was altered to form a cube; (c) plane lights were used to illuminate the apparatus better; (d) having a fixed black background. The maximal distortion factor of lens is -0.1 % in specified field of view (165 mm (H) × 124 mm (V)). So the accuracy of deformation measurement is less affected by lens distortion. The physical size of each pixel of CMOS camera is 5.2 μm × 5.2 μm. The accuracy of recording measurement in *X* and *Y* directions is identical.

Digital image measurement technique of sub-pixel corner locator can measure sample deformation by capturing displacement of corners of white square shape on black rubber membrane, as shown in Fig. 1(a). This method yields more data while measuring axial and radial deformation of samples and accuracy is also relatively high. Precision analysis shows that both axial and radial accuracy of measurement is 2 % of pixels and the strain measurement accuracy is 10^{-4} [7].
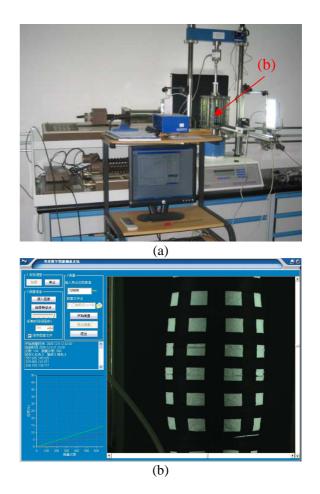

(a)

(b)

Figure 1. Unsaturated soil triaxial test system based on digital image measurement technology.

2.2 Principle of measurement

Figure 2 shows the distribution of corners within the measured sample region during the triaxial test. Radial strain, axial strain as well as estimated volumetric strain can be calculated by the pixel coordinates of corners. The corners data can not be used to calculate the strain on the curved surface of sample because the deformation of curved surface is not plane deformation. Only the corners of radial edge and two axial terminal of measured sample region may be used to calculate strain. These corners must be laid in an identity plane and the object distances to lens should be the same.

The unit of original test data is pixel when the digital image measurement method is used in the test. The test data of pixel unit does not need to be converted to physical value of SI (International System of Units) when we calculate the strain, because the strain is a relative deformation quantity.
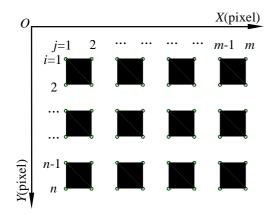
_____

Figure 2. Distribution of corner location.

But the test data must be of physical value of SI when we calculate the void ratio, which can be derived from the conversion by the definitive pixel equivalent (physical length per pixel).

The axial strain of samples at any time during the experiment can be acquired as follows: 1) calculate all *Y*-coordinate difference of two terminal corners on identical axes; 2) calculate their ratios of axial length increment to initial value based on first step; 3) calculate this time axial strain, i.e. average value of these ratios. So the mean axial strain of *t* time is given as:

$$\varepsilon_a^t = \frac{1}{m} \sum_{j=1}^{m} \frac{(Y_{nj}^0 - Y_{1j}^0) - (Y_{nj}^t - Y_{1j}^t)}{(Y_{nj}^0 - Y_{1j}^0)} . \qquad (1)$$

For the radial strain of samples at any time, the calculation procedure is the same as the axial strain, as follows: 1) calculate all *X*-coordinate difference of two edge corners in the same radial section; 2) calculate their ratios of radial diameter increment to initial value based on 1); 3) calculate axial strain, i.e. average value of these ratios. So the mean radial strain of *t* time can be expressed as:

$$\varepsilon_r^t = \frac{1}{n} \sum_{i=1}^{n} \frac{(X_{im}^0 - X_{i1}^0) - (X_{im}^t - X_{i1}^t)}{(X_{im}^0 - X_{i1}^0)} . \qquad (2)$$

Calculation of volumetric strain is based on elementary hypotheses that the sample deformation is isotropic. Figure 3 shows that the calculation method of *t* time volumetric strain. To be specific: 1) measured section is separated into many micro truncated cone; 2) calculate calculating volume of every micro truncated cone; 3) sum the volume of all micro truncated cones to calculate total volume

of the measured section; 4) calculate their ratios of volume increment to initial volume; 5) calculate *t* time volumetric strain, i.e. average value of these ratios. So the mean volumetric strain of *t* time can be acquired based on Eq. (3), Eq. (4) and Eq. (5):

$$V^0 = \frac{\pi}{8} \left[\frac{1}{n} \sum_{i=1}^{n} (X_{im}^0 - X_{i1}^0) \right]^2 \qquad (3)$$
$$\cdot [(Y_{n1}^0 - Y_{11}^0) + (Y_{nm}^0 - Y_{1m}^0)]$$

$$V^t = \frac{\pi}{24} \sum_{i=1}^{n-1} [(X_{im}^t - X_{i1}^t)^2 + (X_{im}^t - X_{i1}^t)$$
$$\cdot (X_{(i+1)m}^t - X_{(i+1)1}^t) + (X_{(i+1)m}^t - X_{(i+1)1}^t)^2] \qquad (4)$$
$$\cdot [(Y_{(i+1)1}^t - Y_{i1}^t) + (Y_{(i+1)m}^t - Y_{im}^t)]$$

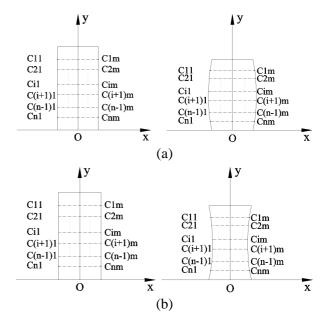$$\varepsilon_v^t = \frac{V^t - V^0}{V^0} . \qquad (5)$$

(a)

(b)

Figure 3. Distribution of corner location before and after suction-controlled triaxial tests: (a) Triaxial and (b) Isotropic compression.

We need to adjust the computational procedure of the strain to the specific measured section of samples in each test. The deformation of the whole sample can be measured together based on the local deformation. The end restraint has been lessened in the middle 1/3 section of the sample [8-10], making it suitable for measurement of local deformation. The stress distribution of this section is also fairly uniform, when the deformation is large enough.

_____

3 Deformation measurement of the unsaturated soil sample

3.1 Test equipment and soil sample

Local deformation measurement of soil sample can avoid the effect of end restraint on sample deformation in soil triaxial test, and digital image measurement method provides a simple and convenient way to study both saturated and unsaturated soils. In this paper, we applied the method based on digital image measurement for sample deformation measurement in suction-controlled unsaturated soil triaxial compression test. The test equipment included refitted Unsaturated Soil Triaxial Test System, GDS Company (UK) and the Digital Image Measurement System developed in the research lab at Dalian University of Technology [8]. The soil used in the tests was silty clay. The average content of sand, silt and clay was 2.39 %, 95.61 %, and 2 %, respectively. Samples (80 mm in height and 39.1 mm in diameter), were prepared using in-place and quintuplicate layers tamping compaction. Each layer was compacted at a moisture content of 4 % less than the optimum moisture content. The tamping compaction corresponds to a compactive effort considerably less than the standard Proctor, and resulted in an average dry density of 1.73 g/cm^3, along with an average moisture content of 13.9 %. Table 1 shows physical properties of the compacted soil.

3.2 Tests content

A series of 2 drained (constant-s) isotropic loading and triaxial compression tests were conducted in suction-controlled unsaturated soil triaxial test apparatus on 2 identically prepared samples of compacted soil. In each case, an isotropic consolidation (net mean stress $p=(\sigma_1+2\sigma_3)/3-u_a$ ranging from 10 kPa to 310 kPa) followed the

equalization of the pore fluids (air and water) for the pre-established value of matric suction $s=u_a-u_w$ (s=50 kPa and 150 kPa).

Next, a triaxial compression under suction-controlled and p=310 kPa. In the isotropic consolidation test, a constant rate of $\Delta p/\Delta t$=6 kPa/h (approximately, 1 kPa load increment every 10 min) was applied. In the suction-controlled triaxial test, loading velocity $v = 0.006$ mm/min was used. Deformations of overall and middle 1/3 sample were simultaneously measured during the test.

3.3 Results and Analyses

Figure 4 shows the specific volume $v = 1+e$ versus net mean stress p response of the compacted soil samples during the isotropic consolidation stage. In the tests conducted at s=50 kPa and 150 kPa, the test results show that the deformation trends of overall and middle 1/3 sample are fairly similar under the isotropic compression stage, but deformation of the former less than the latter under the same net mean stress. This suggested that end restraint is not significant to middle 1/3 sample compared with the overall sample. The deformation of middle 1/3 sample is much more sufficient.

3.4 Triaxial compression tests

Figures 5 and 6 show axial strain ε_a, radial strain ε_r versus deviatoric stress $q=\sigma_1-\sigma_3$ and volumetric strain ε_v versus axial strain ε_a response of the compacted soil samples during the triaxial compression stage. In the tests conducted for initial net mean stress $p_{ini} = 310$ kPa under $s = 50$ kPa and 150 kPa, the test results in Fig. 5 show that the deviatoric stress of the latter is greater than the former under the same axial or radial strain whether test results of overall sample or middle 1/3 sample, but volumetric strain of the former is greater than the latter when axial strain is the same. These tests

Table 1. Physical properties of compacted soil.

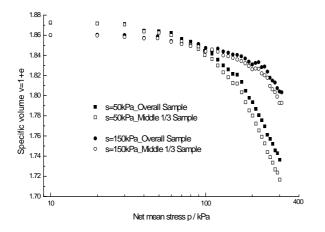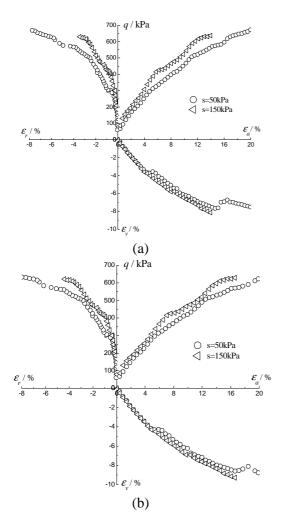| Grain size distribution			w/%	ρ /(g·cm^{-3})	Limit moisture content			G_s	ρ_{dmax} /(g·cm^{-3})	w_{opt} /%
Sand>0.075 mm) / %	Silt 0.075-0.005 mm / %	Clay<0.005 mm / %			w_P/%	w_L/%	I_P/%			
2.39	95.61	2	13.9	1.45	18.2	32.4	14.2	2.73	1.73	17.8

Figure 4. Curve of v=1+e~p of overall and middle 1/3 sample unsaturated soil in isotropic stresses under s=50 kPa and s=150 kPa.

indicate that suction has a significant effect on the shearing strength of unsaturated soil and that will be enhanced with suction increasing.

The test results of identity suction show that both axial and radial strain of middle 1/3 sample are greater than the overall sample under the same deviatoric stress and volumetric strain of the former is also greater than the latter, Fig. 6. These test results further indicate that the end restraint has less effect on middle 1/3 sample so that it can deform sufficiently and the test results are consistent with real properties of the samples.
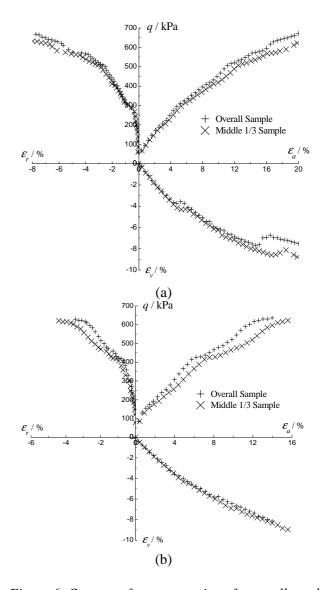

(a)

(b)

Figure 5. Curves of stress-strain in unsaturated soil triaxial compression test for $p_{ini}=310$ kPa: (a) overall sample and (b) middle 1/3 sample.

(a)

(b)

Figure 6. Curves of stress-strain of overall and middle 1/3 sample unsaturated soil in triaxial tests for $p_{ini}=310$ kP: (a) s=50 kPa and (b) s=150 kPa.

_____

4   Conclusions

A series of constant-*s* isotropic loading and triaxial compression tests were conducted on compacted soil, using the digital image measurement method. Our experimental studies indicated that digital image measurement method provides a simple and convenient way for deformation measurement of samples in suction-controlled unsaturated soil triaxial test. The results suggested that the measurement system can correct the overestimation of overall sample deformation caused by the end restraint. The end restraint was lessened at the middle 1/3 sample and the test results in this area can largely represent the real properties of deformation of samples, providing more reliable data for constitutive relationship study of unsaturated soil.

Acknowledgments

References

[1]   Chen Z.H., Sun S.G., Fang X.W. and et al.: *Recent advances of the measuring technology for unsaturated soils and special soils*, Chinese Journal of Geotechnical Engineering, 28 (2006) 2, 147-169.

[2]   Dong J.J. and Shao L.T.: *Critical state surface in p-q-s stress space based on deformation of middle part of specimens*, Chinese Journal of Geotechnical Engineering, 31 (2009) 10, 1607-1 613.

[3]   Shao L.T., Wang Z.P., and Han G.C.: *Digital image processing technique for measurement of the radial deformation of specimen in triaxial test*, Chinese Journal of Geotechnical Engineering, 23 (2001) 3, 337-341.

[4]   [4] Wang Z.P., Shao L.T. and Liu Y.L.: *Error and accuracy analyses of digital image processing technique for measuring specimen deformation in triaxial test*, Journal of Dalian University of Technology, 42 (2002) 1, 98-103.

[5]   [5] Shao L.T., Dong J.J., Liu Y.L. and Sun Y.Z.: *Digital image measurement method of measuring triaxial specimen deformation based on sub-pixel accurate corner locator*, Rock and Soil Mechanics, 29 (2008) 5, 1329-1333.

[6]   [6] Stock C., Mühlmann U., Chandrakerm M.K. and Pinz A.: *Sub-pixel Corner Detection for Tracking Applications using CMOS Camera Technology*, 26th Workshop of the Austrian Association for Pattern Recognition (ÖAGM/AAPR), Graz Austria, September 2002, 191-199.

[7]   [7] Vaidyanathan P., Malhotra N. and Nayak J.: *A new encryption technique for the secured transmission and storage of text information with medical images*, Engineering Review, 32 (2012) 1, 57-63.

[8]   [8] Dong J.J., Shao L.T., Liu Y.L. and Yao T.: *Measurement of deformation of unsaturated compacted soil triaxial specimen based ondigital image measurement method*, Rock and Soil Mechanics, 29 (2008) 6, 1618-1622.

[9]   Dong J.J., Shao L.T.: *Study of unsaturated compacted soil considering influence of end effect by triaxial test*, Chinese Journal of Rock Mechanics and Engineering, 29(2010)9, 1937-1944.

[10]   Liu L., Li S., Zhang H., Zhang C. and Jia Z.: *Eigenfaces and identification of colour face images*, Computer Modelling and New Technologies, 17 (2013) 4, 136-141.